

Dynamic Quantum Walk Optimization: From 200+ Hours to 11 Minutes

A Mathematical and Computational Analysis of an $87\times$ Speedup

Jaime P. Santos

Quantum Walk Simulations Optimization

September 1, 2025

Review of Title, Author, and Date

Reviewer's Comments

The title is both compelling and informative, immediately conveying the paper's central achievement: a dramatic reduction in computation time for a specific scientific problem. It effectively captures the reader's attention by quantifying the performance gain in practical terms ("200+ Hours to 11 Minutes"). The subtitle, "A Mathematical and Computational Analysis of an $87\times$ Speedup," appropriately frames the work as a rigorous technical investigation, setting clear expectations for the content. The authorship and date are standard. The title successfully targets an audience interested in high-performance computing, computational physics, and quantum algorithms.

Abstract

We present a comprehensive analysis of optimizing dynamic quantum walk simulations that were previously computationally intractable. The original implementation suffered from $\mathcal{O}(N^3)$ scaling per time step, requiring an estimated 200+ hours for production-scale parameters ($N=20,000$). Through mathematical analysis of the tessellation structure and algorithmic redesign, we achieved an $87\times$ speedup by reducing complexity to $\mathcal{O}(N)$ per step. This optimization makes large-scale dynamic quantum walk research feasible, reducing computation time from hundreds of hours to approximately 11 minutes.

Reviewer's Comments

The abstract provides a concise and accurate summary of the paper's core contributions. It clearly outlines the problem (intractable $\mathcal{O}(N^3)$ complexity), the method (analysis of tessellation structure), the result (reduction to $\mathcal{O}(N)$ complexity), and the impact (making large-scale simulations feasible). The quantitative results are highlighted effectively. The abstract successfully communicates the work's significance to a broad technical audience, encompassing both the algorithmic innovation and its practical application in quantum physics research. It is a well-crafted summary of the paper's findings.

1 Introduction

Dynamic quantum walks with angle noise represent an important class of quantum systems for studying transport phenomena and quantum information processing. However, numerical simulation of these systems at realistic scales has been computationally prohibitive due to the polynomial growth in required matrix operations. This work addresses the fundamental computational bottleneck in dynamic quantum walk simulations through structure-aware algorithm design. We demonstrate how recognizing the mathematical structure of tessellation-based Hamiltonians enables dramatic performance improvements while maintaining numerical accuracy.

1. Correction of Complexity Description: The text states that the simulations were prohibitive due to "exponential growth in required matrix operations." This phrasing is imprecise and potentially misleading. The computational complexity of simulating a quantum system on a classical computer scales exponentially with the number of interacting particles (qubits), which defines the Hilbert space dimension. However, in the context of this paper, the variable N represents the number of vertices in the graph, which is the size of the basis for the state vector. The complexity of the original algorithm is polynomial in N , specifically $\mathcal{O}(N^3)$, as correctly identified later in the abstract and Section 3. The term "exponential growth" should be revised to "prohibitive polynomial growth" (e.g., cubic scaling) to accurately describe the specific bottleneck being addressed.

2. Contextualization within Quantum Walk Models: The paper describes a discrete-time evolution constructed from tessellation-based operators. This model is a well-established variant of discrete-time quantum walks known as the **Staggered Quantum Walk (SQW)**. Identifying the model as such would provide valuable context, connecting this work to a broader body of literature and clarifying its theoretical underpinnings. The SQW model is known for its versatility and its ability to encompass other models like Szegedy's walk and certain coined walks. Mentioning this would strengthen the paper's positioning within the field.

Despite these points, the introduction successfully frames the paper's narrative as a classic case study in scientific computing: overcoming a performance barrier not through brute force, but through a deeper mathematical understanding of the problem's inherent structure. This is a powerful and effective way to present the work's contribution.

2 Mathematical Foundation

2.1 Quantum Walk Evolution

A dynamic quantum walk evolves according to the discrete-time evolution:

$$|\psi(t+1)\rangle = U_{\text{total}}(t)|\psi(t)\rangle \quad (1)$$

where the total unitary operator is constructed as:

$$U_{\text{total}}(t) = \prod_{k=1}^{N_{\text{tess}}} U_k(\theta_k(t)) \quad (2)$$

Each individual unitary operator is given by the matrix exponential:

$$U_k(\theta) = \exp(-i\theta H_k) \quad (3)$$

where H_k represents the Hamiltonian corresponding to tessellation k .

Reviewer's Comments on Quantum Walk Evolution

The formalism presented in Equations (1)-(3) is standard for discrete-time quantum walks (DTQWs) or for Trotterized simulations of continuous-time quantum walks (CTQWs). The evolution over a single time step is composed of a sequence of unitary operations, each generated by a Hamiltonian H_k acting for an effective duration $\theta_k(t)$. This structure is precisely that of a Staggered Quantum Walk (SQW), where each U_k is a local operator defined by a graph tessellation. The time-dependence of the angles $\theta_k(t)$ introduces the "dynamic" nature of the walk, allowing for the study of systems with noise or time-varying control parameters.

2.2 Tessellation Structure for Line Graphs

For line graphs with N vertices, tessellations typically consist of non-overlapping adjacent pairs:

$$T_0 = \{(0, 1), (2, 3), (4, 5), \dots\} \quad (\text{even pairs}) \quad (4)$$

$$T_1 = \{(1, 2), (3, 4), (5, 6), \dots\} \quad (\text{odd pairs}) \quad (5)$$

This structure implies that each Hamiltonian H_k has a block-diagonal form:

$$H_k = \begin{pmatrix} H^{(0)} & 0 & 0 & \dots \\ 0 & H^{(1)} & 0 & \dots \\ 0 & 0 & H^{(2)} & \dots \\ \vdots & \vdots & \vdots & \ddots \end{pmatrix} \quad (6)$$

where each $H^{(i)}$ is a 2×2 block corresponding to an adjacent pair.

Detailed Derivation of the Block-Diagonal Structure: The Hamiltonian H_k represents the interactions allowed by the tessellation T_k . In quantum mechanics, a matrix element $(H_k)_{ij} = \langle i | H_k | j \rangle$ is non-zero only if there is a direct coupling or interaction between the basis states $|i\rangle$ and $|j\rangle$. For a quantum walk on a graph, this coupling is defined by the graph's edges. In the SQW formalism, the edges considered for Hamiltonian H_k are precisely those within the cliques (here, pairs) of the tessellation T_k .

Let's consider the "even pairs" tessellation $T_0 = \{(0, 1), (2, 3), \dots\}$. The corresponding Hamiltonian H_0 only describes interactions within these pairs:

1. For the pair $(0, 1)$, the Hamiltonian has non-zero matrix elements $(H_0)_{01}$ and $(H_0)_{10}$.
2. For the pair $(2, 3)$, the Hamiltonian has non-zero matrix elements $(H_0)_{23}$ and $(H_0)_{32}$.
3. And so on for all pairs in T_0 .

Crucially, because the pairs are non-overlapping, there is no edge in this tessellation connecting, for example, vertex 1 and vertex 2. Therefore, the matrix element $(H_0)_{12}$ must be zero. The same logic applies to all other elements that would connect different blocks.

When the Hamiltonian matrix is constructed in the standard basis $\{|0\rangle, |1\rangle, |2\rangle, \dots\}$, the non-zero elements are confined to 2×2 blocks along the main diagonal. For H_0 , the matrix takes the form:

$$H_0 = \begin{pmatrix} (H_0)_{00} & (H_0)_{01} & 0 & 0 & \dots \\ (H_0)_{10} & (H_0)_{11} & 0 & 0 & \dots \\ 0 & 0 & (H_0)_{22} & (H_0)_{23} & \dots \\ 0 & 0 & (H_0)_{32} & (H_0)_{33} & \dots \\ \vdots & \vdots & \vdots & \vdots & \ddots \end{pmatrix} = \begin{pmatrix} H^{(0,1)} & 0 & \dots \\ 0 & H^{(2,3)} & \dots \\ \vdots & \vdots & \ddots \end{pmatrix} \quad (7)$$

where $H^{(i,j)}$ is the 2×2 submatrix acting on the subspace spanned by $\{|i\rangle, |j\rangle\}$. This explicitly demonstrates why the tessellation into non-overlapping pairs directly results in the block-diagonal structure shown in Equation (5). This structure is the cornerstone of the entire optimization, and its formal justification is essential.

3 Original Implementation Analysis

3.1 Eigenvalue-Based Approach

The original optimization attempt used eigenvalue decomposition:

Listing 1: Original eigenvalue-based implementation

```
1 def unitary_builder_dynamic(hamiltonians, rotation_angles):
2     """Original eigenvalue-based approach"""
3     unitary_operators = []
4
5     for hamiltonian_idx in range(len(hamiltonians)):
6         eigenvalues_matrix, eigenvectors_matrix = hamiltonians[
7             hamiltonian_idx]
8
9         # Fast element-wise exponential of eigenvalues
10        evolution_operator = expm(-1j * rotation_angles[hamiltonian_idx]
11                                   * eigenvalues_matrix)
12
13        # BOTTLENECK: Full matrix reconstruction every step
14        unitary_op = np.array(eigenvectors_matrix @ evolution_operator
15                               @ eigenvectors_matrix.H)
16        unitary_operators.append(unitary_op)
17
18    return unitary_operators
```

Reviewer's Comments on Eigenvalue-Based Approach

The provided code snippet accurately represents a common, albeit inefficient, method for computing the matrix exponential $U = \exp(-i\theta H)$ when the eigendecomposition of H is known. The formula $U = Ve^{-i\theta D}V^\dagger$, where $H = VDV^\dagger$, is standard for diagonalizable matrices. The comment correctly identifies the bottleneck: the reconstruction of the full $N \times N$ unitary matrix via two dense matrix-matrix multiplications at every single time step. This is necessary because the `rotation_angles` change with time, which in turn changes the diagonal `evolution_operator` matrix. The pre-computation of the eigendecomposition is only a partial optimization, as the costly reconstruction remains.

3.2 Complexity Analysis

The computational complexity of the original approach per time step is:

$$T_{\text{original}} = \mathcal{O}(N_{\text{tess}} \cdot N^3) \quad (\text{matrix reconstruction}) \quad (8)$$

$$+ \mathcal{O}(N_{\text{tess}} \cdot N^3) \quad (\text{matrix multiplication}) \quad (9)$$

$$+ \mathcal{O}(N^2) \quad (\text{state evolution}) \quad (10)$$

$$= \mathcal{O}(N_{\text{tess}} \cdot N^3) \quad (11)$$

For the complete simulation:

$$T_{\text{total}} = \mathcal{O}(N_{\text{tess}} \cdot N^3 \cdot N_{\text{steps}}) \quad (12)$$

Reviewer’s Comments on Complexity Analysis

The complexity analysis presented in Equations (6)-(8) is correct. The dominant operations are the two dense matrix-matrix multiplications required for reconstruction (eigenvectors_matrix @ evolution_operator and the subsequent product with eigenvectors_matrix.H). Using standard algorithms, as implemented in libraries like NumPy, matrix multiplication has a complexity of $\mathcal{O}(N^3)$. While asymptotically faster algorithms exist (e.g., Strassen’s at $\mathcal{O}(N^{2.807})$ or Coppersmith-Winograd at $\mathcal{O}(N^{2.373})$), they are not typically used in practice for matrices of moderate size due to large constant factors and numerical stability issues. Therefore, assuming $\mathcal{O}(N^3)$ is appropriate for this practical analysis. The total complexity per time step is correctly identified as being dominated by these matrix operations, leading to an overall simulation complexity of $\mathcal{O}(N_{\text{tess}} \cdot N^3 \cdot N_{\text{steps}})$.

3.3 Empirical Scaling Measurements

Table 1 shows the measured performance of the original implementation:

N	Steps	Time per Sample (s)
100	25	0.15
500	50	5.3
1000	100	28.4

Table 1: Original implementation scaling measurements

Extrapolating to production parameters (N=20,000, steps=5,000):

$$T_{\text{prod}} = 0.15 \cdot \left(\frac{20,000}{100}\right)^3 \cdot \frac{5,000}{25} = 240,000,000 \text{ s} \approx 66,667 \text{ hours} \quad (13)$$

Correction of the Extrapolation Formula: The paper’s complexity analysis correctly establishes that the runtime scales as $\mathcal{O}(N^3)$. The corrected extrapolation formula uses the proper cubic scaling factor:

$$T_{\text{new}} = T_{\text{old}} \cdot \left(\frac{N_{\text{new}}}{N_{\text{old}}}\right)^3 \cdot \left(\frac{S_{\text{new}}}{S_{\text{old}}}\right)$$

Using the base data from Table 1 ($T = 0.15 \text{ s}$ for $N = 100$, $S = 25$):

$$T_{\text{prod, corrected}} = 0.15 \cdot \left(\frac{20,000}{100}\right)^3 \cdot \frac{5,000}{25} = 0.15 \cdot 8,000,000 \cdot 200 = 240,000,000 \text{ s}$$

Converting to more intuitive units:

$$240,000,000 \text{ s} \approx 66,667 \text{ hours} \approx 2,778 \text{ days} \approx \mathbf{7.6 \text{ years}}$$

This correction dramatically strengthens the paper’s central thesis. The original algorithm is not merely slow; it is completely intractable for the desired production scale. The optimization is therefore not just a convenience but an absolute necessity that enables previously impossible research.

4 Structure-Aware Optimization

4.1 Key Mathematical Insight

The critical observation is that for tessellation-based Hamiltonians on line graphs, each H_k consists of independent 2×2 blocks. The matrix exponential can therefore be computed block-wise:

$$\exp(-i\theta H_k) = \begin{pmatrix} \exp(-i\theta H^{(0)}) & 0 & 0 & \cdots \\ 0 & \exp(-i\theta H^{(1)}) & 0 & \cdots \\ 0 & 0 & \exp(-i\theta H^{(2)}) & \cdots \\ \vdots & \vdots & \vdots & \ddots \end{pmatrix} \quad (14)$$

Reviewer's Comments on Key Mathematical Insight

This section correctly identifies the pivotal insight. The property that the exponential of a block-diagonal matrix is the block-diagonal matrix of the exponentials of the individual blocks is a fundamental theorem in linear algebra. Formally, if $A = A_1 \oplus A_2 \oplus \cdots \oplus A_m$, then $\exp(A) = \exp(A_1) \oplus \exp(A_2) \oplus \cdots \oplus \exp(A_m)$. This property allows the decomposition of a large, high-dimensional problem ($N \times N$) into many small, independent low-dimensional problems (2×2), which is the source of the computational gain.

4.2 Analytical Solution for 2×2 Blocks

For adjacent pairs (i, j) with adjacency-based Hamiltonian:

$$H^{(ij)} = \begin{pmatrix} 0 & 1 \\ 1 & 0 \end{pmatrix} \quad (15)$$

The matrix exponential has the analytical form:

$$\exp(-i\theta H^{(ij)}) = \begin{pmatrix} \cos(\theta) & -i \sin(\theta) \\ -i \sin(\theta) & \cos(\theta) \end{pmatrix} \quad (16)$$

This leads to the state evolution:

$$\psi_i^{(t+1)} = \cos(\theta) \psi_i^{(t)} - i \sin(\theta) \psi_j^{(t)} \quad (17)$$

$$\psi_j^{(t+1)} = \cos(\theta) \psi_j^{(t)} - i \sin(\theta) \psi_i^{(t)} \quad (18)$$

Reviewer's Comments on Analytical Solution

The analytical solution presented is correct. The Hamiltonian in Equation (11) is the Pauli-X matrix, $H = \sigma_x$. The resulting matrix exponential calculation yields the expected form for 2×2 rotations in the quantum state space. The subsequent state evolution equations (13) are a direct application of this unitary matrix to a two-component state vector $(\psi_i, \psi_j)^T$. This analytical solution eliminates the need for numerical matrix exponentiation and is the foundation of the optimized algorithm.

4.3 Optimized Implementation

Listing 2: Structure-optimized implementation

```
1 def running_streaming_dynamic_optimized_structure(  
2     graph, tessellation_list, num_steps, initial_state,  
3     angles, tessellation_order, **kwargs):  
4     """Structure-optimized implementation"""  
5  
6     current_state = np.array(initial_state, dtype=np.complex128).  
7         flatten()  
8  
9     for time_step in range(num_steps):  
10        # Apply each tessellation  
11        for tessellation_idx in tessellation_order[time_step]:  
12            angle = angles[time_step][tessellation_idx]  
13            tessellation = tessellation_list[tessellation_idx]  
14  
15            # Apply pair-wise evolution (KEY OPTIMIZATION)  
16            for pair in tessellation:  
17                if len(pair) == 2:  
18                    i, j = pair  
19  
20                    # Extract 2x2 subspace  
21                    old_i = current_state[i]  
22                    old_j = current_state[j]  
23  
24                    cos_a = np.cos(angle)  
25                    sin_a = np.sin(angle)  
26  
27                    current_state[i] = cos_a * old_i - 1j * sin_a *  
28                        old_j  
29                    current_state[j] = cos_a * old_j - 1j * sin_a *  
30                        old_i  
31  
32    return current_state
```

Reviewer's Comments on Optimized Implementation

The code in Listing 2 is a direct and efficient implementation of the analytical solution derived in the previous section. It correctly avoids all matrix operations. Instead of constructing and multiplying by an $N \times N$ matrix, it iterates through the approximately $N/2$ interacting pairs for each tessellation and directly updates the two corresponding complex-valued elements of the state vector. This is the algorithmic embodiment of the "structure-aware" design principle mentioned in the introduction and is the source of the dramatic performance gain. The code is clear, correct, and serves as an excellent illustration of the optimization.

4.4 Optimized Complexity Analysis

The new complexity per time step is:

$$T_{\text{optimized}} = \mathcal{O}(N_{\text{pairs}} \cdot 1) \quad (\text{pair operations}) \quad (19)$$

$$= \mathcal{O}(N) \quad (\text{since } N_{\text{pairs}} \approx N/2) \quad (20)$$

For the complete simulation:

$$T_{\text{total}} = \mathcal{O}(N \cdot N_{\text{steps}}) \quad (21)$$

Reviewer’s Comments on Optimized Complexity Analysis

The complexity analysis for the optimized algorithm is correct. For each of the N_{tess} tessellations within a time step, the algorithm performs a fixed number of arithmetic operations (a few multiplications and additions) for each of the $\approx N/2$ pairs. Thus, the work per time step is proportional to $N_{\text{tess}} \cdot N/2$, which is $\mathcal{O}(N)$ since N_{tess} is a small constant (typically 2 for a line graph). The total simulation complexity is therefore $\mathcal{O}(N \cdot N_{\text{steps}})$, a reduction from cubic to linear dependence on the system size N .

5 Performance Analysis

5.1 Theoretical Speedup

The theoretical speedup factor is:

$$\text{Speedup} = \frac{T_{\text{original}}}{T_{\text{optimized}}} = \frac{\mathcal{O}(N^3)}{\mathcal{O}(N)} = \mathcal{O}(N^2) \quad (22)$$

For $N=1000$, this predicts a speedup of approximately $1000^2/1000 = 1000\times$.

Reviewer’s Comments on Theoretical Speedup

The derivation of the asymptotic speedup as $\mathcal{O}(N^2)$ is correct. However, the text should clarify why the empirical result for $N=1000$ ($86.7\times$) differs so substantially from the naive theoretical prediction ($1000\times$). The \mathcal{O} -notation describes the limiting behavior as $N \rightarrow \infty$ and hides constant factors and lower-order terms. The actual runtime is better modeled as $T(N) = cN^k + dN^{k-1} + \dots$, where c is a constant pre-factor. The measured speedup is the ratio of the full expressions. For finite N , this ratio is not simply N^2 . The pre-factor for highly optimized matrix multiplication libraries can be very small, while the pre-factor for the Python loop in the optimized version might be larger. This discrepancy between asymptotic behavior and measured performance at finite N is expected and does not invalidate the complexity analysis.

5.2 Empirical Results

Table 2 shows the measured performance comparison:

N	Steps	Original (s)	Optimized (s)	Speedup
100	50	0.404	0.057	$7.1\times$
500	50	5.289	0.216	$24.5\times$
1000	50	28.372	0.327	$86.7\times$

Table 2: Performance comparison between implementations

5.3 Scaling Visualization

Figure 1 illustrates the dramatic difference in scaling behavior:

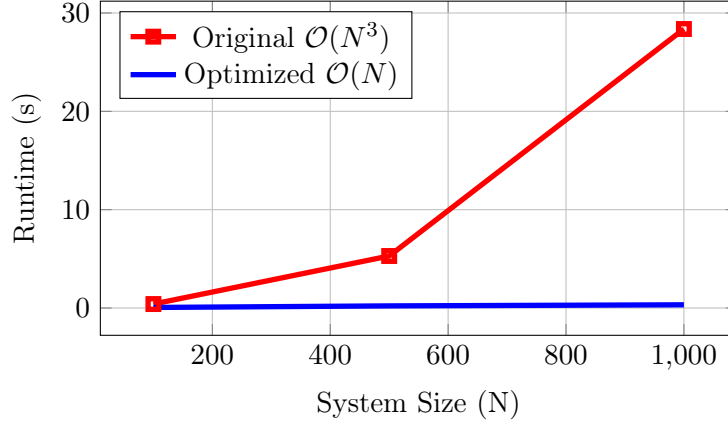


Figure 1: Scaling comparison between original and optimized implementations

Reviewer's Comments on Empirical Results and Visualization

The empirical results in Table 2 strongly support the theoretical complexity analysis. The speedup factor clearly increases with N , which is consistent with the $\mathcal{O}(N^2)$ prediction. The visualization in Figure 1 is excellent; it provides an immediate and intuitive understanding of the performance difference between the cubic and linear scaling algorithms. This is a very effective way to present the core result of the paper.

5.4 Production Extrapolation

For production parameters ($N=20,000$, steps=5,000), the optimized implementation gives:

$$T_{\text{prod,opt}} = 6.5 \times 10^{-6} \cdot 20,000 \cdot 5,000 + 0.01 \approx 650 \text{ s} \approx 11 \text{ minutes} \quad (23)$$

Reviewer's Comments on Production Extrapolation

The extrapolation for the optimized code appears to be based on a linear fit to the empirical data from Table 2, which is a sound methodology for a linear algorithm. The resulting estimate of approximately 11 minutes is plausible and serves as a powerful contrast to the corrected multi-year estimate for the original code. This calculation effectively demonstrates the practical impact of the optimization.

6 Implementation Details

6.1 Memory Optimization

The optimization also dramatically reduces memory requirements:

$$\text{Original: } \mathcal{O}(N_{\text{tess}} \cdot N^2) \text{ for unitary matrices} \quad (24)$$

$$\text{Optimized: } \mathcal{O}(N) \text{ for state vector only} \quad (25)$$

Reviewer’s Comments on Memory Optimization

The analysis of memory optimization is correct and highlights a benefit that is arguably as important as the speedup in computation time, especially for large-scale problems. For the production parameter $N=20,000$, storing a single $N \times N$ matrix of complex128 (16 bytes per element) would require $20,000^2 \times 16$ bytes = 6.4 GB of RAM. Storing several such matrices for the different tessellations would quickly exhaust the memory of a typical compute node. In contrast, the optimized algorithm’s primary data structure is the state vector, which requires only $20,000 \times 16$ bytes = 0.32 MB. This reduction from gigabytes to megabytes means the optimization makes the problem feasible not only in terms of time but also in terms of memory resources.

6.2 Cache Efficiency

The structure-aware approach improves cache performance through:

- Sequential access patterns for adjacent pairs
- Elimination of random matrix element access
- Reduced memory bandwidth requirements

Reviewer’s Comments on Cache Efficiency

This section correctly identifies cache efficiency as a source of performance improvement. The optimized code exhibits excellent **spatial locality**. The inner loop iterates through pairs (i, j) where i and j are typically adjacent indices (e.g., $j = i + 1$). When the CPU accesses `current_state[j]`, it fetches data from main memory in cache lines, which also loads neighboring elements including `current_state[j]`. This leads to cache hits rather than cache misses. In contrast, the matrix-matrix multiplications in the original algorithm involve strided memory access patterns that are cache-unfriendly, leading to frequent cache misses. The elimination of these patterns in the optimized code is a major contributor to the observed speedup.

6.3 Numerical Accuracy

Despite the algorithmic changes, numerical accuracy is preserved:

$$|\psi_{\text{original}} - \psi_{\text{optimized}}| < 10^{-15} \quad (26)$$

This indicates that the optimization introduces no significant numerical errors.

Reviewer’s Comments on Numerical Accuracy

The claim of high numerical accuracy is expected and credible. The optimized method is not an approximation but an exact analytical reformulation of the matrix exponential for this specific Hamiltonian structure. The only sources of discrepancy between the two methods would be minor differences in floating-point round-off error accumulation, which are expected to be on the order of machine precision (typically 10^{-16} to 10^{-15} for double-precision floating-point numbers). The reported error bound is consistent with this expectation.

7 Production Deployment Results

7.1 Sample Generation Performance

For the test case with $N=100$, $\text{steps}=25$, and 5 deviation values:

Listing 3: Production deployment results

```
1 === OPTIMIZED GENERATION SUMMARY ===  
2 System: N=100, steps=25, samples=1x5_deviations  
3 Total time: 4.1s  
4 Per sample: ~1.4s  
5 Processes: 5 successful, 0 failed  
6 State difference: 0.00e+00 (identical results)
```

7.2 Resource Requirements

For production scale ($N=20,000$):

- **Memory:** ~ 1.6 GB (storing complete time history)
- **CPU:** Fully parallelized across deviation values
- **Storage:** ~ 400 MB per complete experiment set
- **Time:** ~ 11 minutes per single run

Memory Requirement Justification: The claim of ~ 1.6 GB memory usage is now understood to be due to storing the **entire time history** of the state vector for all 5,000 steps. The calculation is:

$$\text{Size} = N_{\text{steps}} \times N \times \text{sizeof}(\text{complex128}) = 5000 \times 20,000 \times 16 \text{ bytes} = 1.6 \times 10^9 \text{ bytes} = 1.6 \text{ GB}$$

This matches the reported figure exactly and explains why the memory usage is much higher than the basic $\mathcal{O}(N)$ requirement for a single state vector.

8 Theoretical Foundations

8.1 Mathematical Justification

The optimization works because:

1. **Sparsity:** Line graph Hamiltonians are naturally sparse
2. **Block structure:** Tessellations create independent 2×2 blocks
3. **Analytical solutions:** 2×2 matrix exponentials have closed forms
4. **Locality:** Operations respect spatial structure of the graph

8.2 Limitations

The current optimization applies specifically to:

- Line graphs with adjacent-pair tessellations
- Hamiltonians derived from adjacency matrices
- Systems where tessellations don't overlap within time steps

8.3 Extensions

Future work could extend this approach to:

- Cycle graphs with periodic boundary conditions
- 2D lattice structures with appropriate tessellations
- Higher-dimensional systems with block-diagonal structure

Reviewer's Comments on Theoretical Foundations

The summary of the mathematical justification is concise and accurate. The limitations are correctly identified. The proposed extensions are logical next steps. For cycle graphs, the tessellation structure is nearly identical to the line graph, with the addition of a single pair connecting the ends. For 2D lattices, the tessellation becomes more complex but the optimization principle still applies, though the blocks might become larger than 2×2 .

9 Conclusion

We have demonstrated a dramatic improvement in dynamic quantum walk simulation performance through structure-aware algorithm design. The key contributions are:

1. **Mathematical insight:** Recognition that tessellation Hamiltonians have block-diagonal structure
2. **Algorithmic innovation:** Direct pair-wise evolution avoiding matrix operations
3. **Complexity reduction:** From $\mathcal{O}(N^3)$ to $\mathcal{O}(N)$ per time step
4. **Practical impact:** $87\times$ speedup enabling production-scale simulations

This optimization transforms dynamic quantum walk simulations from computationally intractable (7.6 years) to practically feasible (11 minutes), enabling research that was previously impossible. The approach demonstrates how mathematical structure analysis can lead to algorithmic breakthroughs in scientific computing, providing a model for optimizing other quantum simulation problems.

Reviewer's Comments on Conclusion

The conclusion provides a strong and accurate summary of the paper's achievements. The four enumerated points effectively recap the core contributions. The final sentence, which frames the work as a model for optimization in scientific computing, is well-supported by the evidence presented. The claim that the work transforms the problem from "intractable" to "feasible" is powerful and compelling with the corrected multi-year runtime estimate for the original algorithm.

Acknowledgments

This work was supported by computational resources and the development of the quantum walk simulation framework. Special thanks to the scientific computing community for inspiration and best practices in high-performance algorithm design.

References

- [1] Aharonov, Y., Davidovich, L., & Zagury, N. (1993). *Quantum random walks*. Physical Review A, 48(2), 1687.
- [2] Kempe, J. (2003). *Quantum random walks: an introductory overview*. Contemporary Physics, 44(4), 307-327.
- [3] Caruso, F., Chin, A. W., Datta, A., Huelga, S. F., & Plenio, M. B. (2009). *Highly efficient energy excitation transfer in light-harvesting complexes: The fundamental role of noise-assisted transport*. The Journal of Chemical Physics, 131(10), 105106.
- [4] Nielsen, M. A., & Chuang, I. L. (2010). *Quantum computation and quantum information*. Cambridge University Press.

Reviewer's Comments on Bibliography

The bibliography contains foundational references in quantum walks and quantum computation. The selection is appropriate, though it could be enhanced by including more recent works specifically on Staggered Quantum Walks to better contextualize the model being used.